**Broadened T-cell repertoire diversity in ivIg-treated SLE patients is also related to the individual status of regulatory T-cells**

Nuno Costa[1*], Ana E. Pires[2,13,14*], Ana M. Gabriel[1*], Luiz F. Goulart[1], Clara Pereira[1,3], Bárbara Leal[3], Ana C. Queiros[2], Wahiba Chaara[4,5,6], Maria F. Moraes-Fontes[1,8], Carlos Vasconcelos[7], Carlos Ferreira[8], Jorge Martins[9], Marina Bastos[10], Maria J. Santos[11], Maria A. Pereira[12], Berta Martins[3], Margarida Lima[7], Cristina João[2], Adrien Six[4,5], Jocelyne Demengeot[1], Constantin Fesel[1]

[1]Instituto Gulbenkian de Ciência, Apartado 14, P-2781-901 Oeiras, Portugal
[2]Centro de Estudos de Doenças Crónicas Faculdade de Ciências Médicas, Universidade Nova de Lisboa (CEDOC-FCM-UNL), Rua Prof. Lima Basto, 1099-023 Lisboa, Portugal
[3]Instituto de Ciências Biomédicas Abel Salazar, Largo Prof. Abel Salazar 2, 4099-003 Porto, Portugal
[4]UPMC Univ Paris 06, UMR 7211, F-75013 Paris, France
[5]CNRS Centre National de la Recherche Scientifique, UMR 7211, F-75013 Paris, France
[6]AP-HP, Pitié Salpêtrière Hospital, Service de Biothérapie, F-75013 Paris, France
[7]Hospital de Santo António, Largo Prof. Abel Salazar 2, 4099-003 Porto, Portugal
[8]Hospital de Santa Maria, Av. Prof. Egas Moniz, 1649-035 Lisboa, Portugal
[9]Hospital dos Marmeleiros, Estrada dos Marmeleiros Monte, 9054-535 Funchal, Portugal
[10]Hospital São Teotónio, Av. do Rei D. Duarte, 3504-509 Viseu, Portugal
[11]Hospital Garcia de Orta, Av. Torrado da Silva, 2801-951 Almada, Portugal
[12]Hospital de Faro, Rua Leão Penedo, 8000-386 Faro, Portugal
[13]Grupo de Biologia Molecular, Instituto Nacional de Investigação Agrária e Veterinária, I.P., Estr. do Paço do Lumiar, 22, Ed. S, 1649-038 Lisboa, Portugal
[14]Centro de Biologia Ambiental, Faculdade de Ciências, Universidade de Lisboa, Portugal

[*]These authors contributed equally to the work

Corresponding author: Constantin Fesel, Instituto Gulbenkian de Ciência, Apartado 14, P-2781-901 Oeiras, Portugal. Tel. +351 21 4407900, Fax +351 21 4407970, Email cfesel@igc.gulbenkian.pt

Abstract

Purpose: Intravenous IgG (ivIg) is a therapeutic alternative for lupus erythematosus, the mechanism of which remains to be fully understood. Here we investigated whether ivIg affects two established sub-phenotypes of SLE, namely relative oligoclonality of circulating T-cells and reduced activity of CD4+Foxp3+ regulatory T-cells (Tregs) reflected by lower CD25 surface density.

Methods: We conducted a longitudinal study of 15 lupus patients (14 with SLE and one with discoid LE) treated with ivIg in cycles of 2-6 consecutive monthly infusions. Among these 15 patients, 10 responded to ivIg therapy with clear clinical improvement. We characterized Tregs and determined TCR spectratypes of four Vβ families with reported oligoclonality. Cell counts, cytometry and TCR spectratypes were obtained from peripheral blood at various time points before, during and after ivIg treatment. T-cell oligoclonality was assessed as Vβ-familywise repertoire perturbation, calculated for each patient in respect to an individual reference profile averaged over all available time points.

Results: For 11 out of 15 patients, average Vβ1/Vβ2/Vβ11/Vβ14 repertoires were less perturbed under than outside ivIg therapy. The four exceptions with relatively increased average perturbation during ivIg therapy included three patients who failed to respond clinically to an ivIg therapy cycle. Patients' Treg CD25 surface density (cytometric MFI) was clearly reduced when compared to healthy controls, but not obviously influenced by ivIg. However, patients' average Treg CD25 MFI was found negatively correlated with both Vβ11 and Vβ14 perturbations measured under ivIg therapy.

Conclusions: This indicates a role of active Tregs in the therapeutic effect of ivIg.


Keywords: Systemic Lupus Erythematosus, Autoimmunity, Intravenous IgG, TCR spectratypes, Regulatory T-cells, CD25

Introduction

High-dose intravenous infusion therapy with natural IgG pooled from a large number of donors, termed intravenous immunoglobulin (ivIg), is an effective anti-inflammatory therapy in a variety of autoimmune diseases (1). In patients with Systemic Lupus Erythematosus (SLE) and other forms of lupus, ivIg is not a standard therapy but used as an alternative and complementary therapy that is safe and beneficial for the large majority of treated patients (2, 3). The involved mechanisms, however, are not fully identified. Best documented are Fc receptor-mediated effects (4), particularly involving the inhibitory FcγRIIb (5), but also other mechanisms are likely involved that depend on Fab specificities and idiotypes (1). IvIg can reportedly stimulate T-cells (6-8), and particularly the stimulation of Foxp3+ regulatory T-cells (Tregs), directly demonstrated in cell culture (9), is most likely involved in the beneficial ivIg effects to autoimmunity (10-13). Tregs, which can inhibit the proliferation of activated conventional T-cells and are essential for their regulation (14), are in fact specifically altered in SLE (15), and particularly their reduced surface expression of the high-affinity IL-2 receptor (CD25), likely resulting in impaired functionality (16-18), has been convincingly and repeatedly reported. The possible relevance of Tregs for ivIg therapy, however, has not been systematically investigated so far.

Impaired Treg function leads to deregulated clonal expansion of T-cells and repertoire oligoclonality *in vivo*, as it is most evident in primary Treg deficiencies of mice (19) and humans (20). T-cell oligoclonality can be assessed by studying the diversity of T-cell receptor (TCR) rearrangements, either by assessing the relative usage of TCR Vα or Vβ families, by direct sequencing, or most commonly by spectratyping, i.e. the analysis of size diversity in the CDR3 region that originates from random recombination and imprecise joining of TCR gene segments (21). Such oligoclonality was indeed regularly found in various autoimmune conditions (22-27) and is commonly interpreted as the result of selectively expanded T-cell clones. In SLE, oligoclonal T-cell expansions were found to characterize both the chronic disease per se (28-32) and kidney manifestation (33), although it is not known whether expanded clones were directly pathogenic. Further evidence indicated that these oligoclonal expansions were highly instable during active disease, while not in inactive SLE (32). In order to study TCR diversity under ivIg therapy, here we followed for the first time the longitudinal development of TCR spectratypes in individual patients before, during and after ivIg

therapy, combined with the assessment of Treg properties. We studied 14 SLE patients and one patient with discoid lupus treated with 2-12 consecutive ivIg infusions. Analyzing TCR spectratypes of four Vβ families with alterations in SLE, reported (29), in respect to their time-dependent deviation from individual average profiles, we found that (a) TCR repertoire perturbation, here indicating temporary oligoclonal expansions, was significantly reduced under ivIg therapy when compared with samples from the same patient taken before or after ivIg therapy, and that (b) the individual repertoire perturbation under ivIg was in two out of four studied Vβ families strongly correlated with the individual activity of Foxp3+ Tregs reflected by their average surface CD25 expression.

Methods

Patients and sampling

We studied a total of 15 patients (14 with SLE, 1 with discoid LE) treated with monthly infusions of ivIg with total doses ranging between 400 mg and 2 g per kg body weight, and 16 healthy blood donors as controls. The response to ivIg was assessed in terms of SLEDAI changes and clinical evaluation by the physicians who performed the treatment, and the study was entirely observational and open-label. IvIg was generally added to individually stable base therapies (see Table 1). Approval was obtained from the Ethics Committee of the Portuguese Lupus Patients Association, and all collections were performed after written informed consent. An overview of the patient characteristics and the number of followup samples taken from each patient is given in Table 1. Although patients had disease with different degrees of clinical severity, only one (F6) had active renal involvement but with creatinine levels that always remained normal. Peripheral blood (30 mL per sample) was regularly drawn before each monthly ivIg infusion. In some instances, particularly at the time when a patient received the first ivIg infusion, additional samples were taken at the end of an ivIg infusion, i.e., 1-5 days after the initial sampling.

Flow cytometry

Peripheral blood mononuclear cells (PBMC) were isolated using Vacutainer CPT™ tubes (Becton Dickinson). $1x10^6$ PBMC were then washed twice in PBS containing 2% fetal calf serum, and incubated for 30 min on ice with FITC-anti-CD4 (ebioscience, ref. #11-0049-73), PE/Cy5-anti-CD45RO (Becton Dickinson, ref. #555494) and PE-anti-CD25 (Becton Dickinson, ref. #341011). For intracellular staining, cells were washed again, fixed and permeabilized using a fix/perm kit (ebioscience) according to the manufacturer's instructions, and stained for intracellular Foxp3 with APC-anti-FoxP3 (ebioscience, ref. #45-4776-73). Fluorescence was assessed using a FACScalibur flow cytometer, using unchanged cytometer settings and the CellQuest™ software. For PE-anti-CD25 staining, also the median fluorescence intensity (MFI) was quantified and analyzed in terms of its log transformation (log-MFI). However, not all samples from all patients were stained for CD25, and individual average log-MFIs were calculated from those samples of a given patient where CD25 staining was available.

TCR CDR3 spectratyping

From 5 million PBMC, total RNA was isolated using a commercial kit (E.Z.N.A.®
Blood RNA Kits). From an average of 150 ng total RNA per sample, cDNA was
synthesized by the SuperScriptIII First-Strand Synthesis System for RT-PCR
(Invitrogen). TCR BV(Vβ)-specific spectratypes were then obtained for the TCR CDR3
length distributions of the BV1, BV2, BV11 and BV14 families by the method
described by Pannetier et al. (21). Briefly, synthesized cDNA was used to amplify each
BV family separately. The 25μL PCR mixture contained 0.2mM dNTP (Promega),
2mM $MgCl_2$ (Promega), 0.5μM TCRBV-specific forward primer, 0.2μM TCRBC
reverse primer (5'-CGGGCTGCTCCTTGAGGGGCTGCG-3') and 0.8U *Taq*
polymerase (Promega). Amplification reactions were performed in a MJ Research
PTC100 thermocycler with an initial denaturation step of 94ºC for 4 minutes, followed
by 40 cycles of 94 ºC for 45 seconds, 60 ºC for 45 seconds and 72ºC for one minute. A
final extension step at 72 ºC for 10 minutes was performed. The forward primer
sequences were as follows:
hTCRBV1 (5'-CCGCACAACAGTTCCCTGACTTGC-3');
hTCRBV2 (5'-ACATACGAGCAAGGCGTCGA-3');
hTCRBV11 (5'-GTCAACAGTCTCCAGAATAAGG-3');
hTCRBV14 (5´-GGGCTGGGCTTAAGGCAGATCTAC-3').
The achieved amplicons were then used in a run-off reaction with the labelled reverse
primer hTCRBC-FAM (FAM-5'-ACACAGCGACCTCGGGTGGG-3') in order to label
PCR products, using an initial denaturation step of 94ºC for 4 minutes followed by 5
cycles of 94 ºC for 45 seconds, 60 ºC for 45 seconds and 72ºC for one minute. For the
precise determination of fragment sizes, 2μL of the run-off products in the presence of
the fluorescent size marker ABI Genescan 500 ROX were separated on an automated
ABI 3130XL multicapillary gel system (Perkin Elmer-Applied Biosystems).
Spectratype data were extracted using GeneMapper (v. 3.7, from Applied Biosystems,
CA, USA). Briefly, the software program identified each histogram peak by its PCR-
size length and determined the area under each peak.

Spectratype analysis

Spectratypes of the CDR3 region from an ideal naive repertoire follow an approximate
Gaussian distribution containing eight or more peaks (34). Skewed CDR3 Vβ profiles

can be detected as perturbation of this distribution. Accordingly, we analyzed spectratype data with the ISEApeaks® software package (34, 35). For each Vβ(BV)-familywise CDR3 length profile, the percentage of each peak was quantified by dividing its area by the total area of all detectable peaks within the profile. For each BV family analyzed, individual reference profiles were furthermore computed as the average CDR3 peak distribution of all samples drawn from each respective patient undergoing ivIg therapy. Then, the generalized Hamming distance between the peak profile of each single sample and that of the reference profile for the respective patient was calculated for each BV. This distance was used as perturbation index (36, 37) ranging from 0% (identical profiles) to 100% (complete divergence). For a few samples without any detectable amplification for one but successful amplification of other BV families, perturbation was considered 100% for the non-amplifying family if other samples of the same patient showed amplification in this family. A few other samples that showed low-grade but visible amplification not reaching the detection threshold, as well as all BV1 profiles from three patients where regularly no amplification was detected, were excluded from the analysis.

For individual comparisons of profiles under and outside ivIg therapy, perturbation indices were averaged over the detectable BV families and the respective samples of a given patient either under or outside ivIg treatment. Samples were considered under ivIg if taken at least 25 days after a respective first ivIg infusion. Samples drawn either before the first ivIg infusion of a therapy cycle or at least 45 days after a respective last ivIg infusion were considered outside ivIg treatment. Some samples, particularly those collected immediately after the end of the first ivIg infusion received by a patient, were neither considered under nor outside ivIg treatment, but only taken into account to calculate the individual reference profile. Generalized paired t-tests, according to Rosner's adapted statistic design (38) for the case where paired comparisons consist of variable numbers of multiple observations of each type as it is the case in our study, were calculated for perturbation averages under versus outside ivIg treatment either over the pairings available for a respective BV (12 for BV1 that was undetectable in three patients, and 15 for BV2, BV11 and BV14), or over all 57 available patient- and BV-familywise pairings jointly. The likelihood optimization necessary for Rosner's generalized paired t-test was performed by several consecutive runs of the algorithm 'Amoeba' (39) using the software IgorPro (WaveMetrics). Otherwise we preferentially

used distribution-independent statistical tests: the Mann-Whitney test for group comparisons, and Spearman rank correlation for correlations, which were calculated with accordingly adapted macros on the software IgorPro. Weighted least squares regression was calculated with the lm function implemented in the R statistics package (40), using the square root of the sample number considered per patient as weighting factor. P-values below 0.05 were generally considered significant.

Results

Evolution of TCR CDR3 profiles during ivIg therapy

Immunoscope spectratyping (21) (see methods) was used to examine the size distribution of TCR CDR3 Vβ chain rearrangements in four Vβ families in 15 patients before, during and after ivIg therapy that included six consecutive monthly infusions at dosages indicated for autoimmune disorders (see methods). We selected the Vβ1, Vβ2, Vβ11 and Vβ14 families for our study since they showed the best published evidence for specific alterations and shared oligoclonality in SLE patients (29). Table 1 gives an overview of our studied patients: they were treated with ivIg due to systemic or cutaneous flares, most of them in parallel with corticosteroids and/or cytostatics, and mostly responded well to ivIg. CDR3 size profiles from one exemplary patient are shown in Fig. 1, and analogous profiles for a second patient can be seen in the supplementary figure S1. In Fig. 1, before ivIg therapy and immediately after the first infusion very few peaks can be seen in the profiles of all four Vβ families, indicating high repertoire oligoclonality and severe diversity constraint (Fig. 1, days 0 and 4). During ivIg therapy, it is evident that the rearrangements of all four Vβ families evolved toward a more diverse repertoire characterized by approximately Gaussian-distributed sizes. Thus, the expanded clones that had predominated before the initiation of ivIg infusion (pathogenic or not) either disappeared or were substantially reduced in frequency in all four Vβ families studied during ivIg therapy. Diversified profiles under ivIg were overall individually stable, although they did not always converge to ideal Gaussian distributions, as it can be seen for the Vβ1 family in Fig. 1. Such small but stable deviations, also seen in other patients, likely reflected individual particularities as they have also been reported in healthy control subjects (29). Since we collected consecutive samples from our patients, we defined individual reference profiles by the average of all profiles obtained from each respective patient and Vβ family (instead of an average control group reference profile as it is usually done when repeated measurement are not available). As in previous studies, relative oligoclonality was then described by the perturbation index (36, 37) of each sample and Vβ family, here reflecting the deviation of the spectratype assessed at each time point from the average profile calculated for the same patient: the more a profile deviated from this individual average at a given time point, the more perturbed we considered the TCR repertoire at that time point.

Reduced TCR repertoire perturbation under ivIg therapy

In order to address the question whether ivIg therapy had an effect on TCR repertoire diversity, we compared, for each patient, average perturbations of all detectable Vβ families under and outside ivIg treatment (the latter including time points before and after the treatment period, also see methods). For 11 of the 15 patients studied, average perturbations were lower under ivIg treatment. Nine of these 11 patients had responded to ivIg therapy with clinical improvement. The four exceptions (F2, F4, P150, FA1), in contrast, where the average perturbation was relatively increased during ivIg therapy, included three patients who failed to respond clinically to at least one therapy cycle (F2, F4, P150). The reduced perturbation under ivIg can also be seen for most of the respective pairings for individual Vβ families (Fig. 2).

Accordingly, we tested whether the reduced perturbation under ivIg therapy was statistically significant when considering all patients and all Vβ-families together, by paired comparisons of perturbation averages under versus outside ivIg treatment. For this purpose we used the generalization of the paired t-test for multiple comparisons per pairing (38), which also takes the numbers of each observation type per pairing into account. Calculated on all 4x15-3 patient- and Vβ-familywise pairings (see methods), we found that the difference was clearly significant (P=0.0001), and also when calculated for each individual Vβ separately, it was significant for three out of four (Vβ 1: P=0.02; Vβ 2: P=0.049; Vβ 11: P=0.03). This is further illustrated by Fig. 3, which shows the individual development of all four Vβ-family perturbation scores assessed in six selected patients. Among them, F3, P97, F8 and LI1 (Fig. 3, upper part) represent patients with reduced perturbation under ivIg who also responded successfully to ivIg therapy, while F4 and F2 (Fig. 3, lower part) showed no reduced perturbation and failed to improve clinically during an ivIg therapy cycle. Although a reduction in the perturbation during treatment periods (arrows in Fig. 3) is noticeable in the first group of patients, the dynamics of TCR repertoire perturbation differed between individual patients. While F3 almost immediately diminished perturbation in response to ivIg therapy, F8 reached clearly lower levels only at the end of ivIg therapy. P97, in contrast, showed no visibly increased perturbation before ivIg therapy and displayed little change during therapy, while the perturbation rose in all four Vβ families at the end of the ivIg treatment period. LI1 had two consecutive ivIg infusion cycles (arrows) (for full CDR3

size profiles of this patient, see supplementary figure S1). After a first six-month therapy cycle with little visible change in the TCR repertoire, the patient suffered a clinical relapse before receiving a second cycle of ivIg infusions. It is apparent from Fig. 3 that this relapse (between the arrows) was accompanied by high perturbation in all four Vβ families, which, however, rapidly normalized when the patient resumed ivIg therapy. In the group of patients without clinical improvement, F4 never reduced TCR repertoire perturbation during the ivIg therapy in any family. F2 received two consecutive therapy cycles, motivated as for LI1 by a disease flare that followed the initially successful first cycle (full arrow). When ivIg therapy was resumed, however, it failed to improve the clinical symptoms of the patient and was therefore interrupted after three monthly infusions (dashed arrow). In contrast to LI1, F2 showed no reduction of TCR repertoire perturbation during ivIg treatment.

While reduced repertoire perturbation was clearly visible one month after the first ivIg infusion, samples that we took occasionally immediately after the first infusion were not clearly different from those taken before. A possibly interesting exception was patient FA1, where an individual Vβ1 fragment size virtually disappeared immediately after two consecutive ivIg infusions, but later reappeared (see supplementary fig. S2).

Treg CD25 surface density correlates with lower TCR repertoire perturbation

From the same blood samples used for spectratype analysis, we also stained freshly isolated peripheral blood mononuclear cells (PBMC) for flow cytometry analysis in order to quantify and characterize $CD4^+Foxp3^+$ regulatory T-cells (Tregs). We measured frequencies within total $CD4^+$ T-cells and CD25 surface density represented by median fluorescence intensity (MFI, see methods), for total $CD4^+FoxP3^+$ Tregs and three $CD4^+Foxp3^+$ subpopulations as defined (41), depicted in Fig. 4: $CD45RO^+FoxP3^{hi}$ (activated Treg; R6 in Fig. 4), $CD45RO^+FoxP3^{lo}$ (supposedly nonsuppressive 'non-Treg'; R5), and $CD45RO^-FoxP3^{lo}$ (naive-like 'resting' Treg; R7). Analyzing all $Foxp3^+$ Tregs, we found CD25 MFI, but not $Treg/CD4^+$ frequency, clearly reduced in the patients when compared to healthy controls (Fig. 5). However, these parameters were not evidently influenced by ivIg since comparisons of Treg frequency or CD25 MFI before versus after ivIg were insignificant (not shown, but see supplementary figure S3 for individual changes in CD25 MFI under ivIg). Still, Treg properties of individual patients might influence ivIg effects, and particularly its reduction of TCR repertoire

perturbation. What concerns Treg frequencies, we did not find such an influence (Table 2). Analyzing surface CD25 density, in contrast, we found surprisingly that the patients with relatively high Treg average CD25 MFI also had clearly lower TCR perturbations under ivIg in two out of four studied Vβ families (Vβ11 and Vβ14). This resulted in strong and significant negative correlations that were equally evident in terms of distribution-independent Spearman correlation and calculated by weighted least squares regression, taking the different sample numbers per patient under ivIg into account (Table 2, Fig. 6). Individual differences in Treg CD25 MFI that we found correlated with repertoire perturbation under ivIg were themselves clearly not caused neither demonstrably influenced by ivIg treatment, but rather largely existed already before ivIg initiation and were unrelated to changes under ivIg (supplementary Fig. S3). When analyzing Treg subsets analogously, average CD25 densities in both the CD45RO$^+$FoxP3$^{hi}$ and CD45RO$^+$FoxP3$^{lo}$ subsets showed similar negative correlations with Vβ11 and Vβ14 perturbation. Only in naive/resting CD45RO$^-$ Foxp3$^+$ cells, there was no correlation detected between CD25 surface density and TCR perturbation, as it was also the case for the naïve (CD45RO$^-$) and memory (CD45RO$^+$) subsets of conventional CD4$^+$Foxp3$^-$ T-helper cells (Table 2). In contrast to Vβ11 and Vβ14, the perturbation scored in the Vβ1 and Vβ2 families did not significantly correlate with CD25 surface densities.

Discussion

The adaptive immune system with its specific capacity to eliminate pathogens is based on antigen-specific B- and T-cells. Although the size of specifically responsive T-cell clones can markedly increase upon antigenic stimulation, the number of expanded memory cells resulting from such stimulation is normally very limited and preserves an overall repertoire of high diversity. However, it has been demonstrated that during acute and chronic viral infections the T-cell repertoire can be biased by selective clonal expansions (42-45). Particularly in various immunodeficient conditions, the T-cell repertoire diversity is reduced, and their repair can be monitored by the assessment of TCR diversity, e.g. in immune reconstitution following bone marrow transplantation (46-48) and during antiretroviral therapy of HIV infection (36, 49). In these conditions, where a small number of clones may expand by homeostatic proliferation and yield normal lymphocyte numbers but not a repertoire of normal diversity, the assessment of repertoire diversity is of proven relevance.

Patients with autoimmune disorders also have typical constraints of their lymphocyte repertoire with an overrepresentation of expanded clones. Skewed and oligoclonal T-cell repertoires with persistently expanded clones have been reported in rheumatoid arthritis (22, 24), multiple sclerosis (25), psoriasis vulgaris (26), myasthenia gravis (27), and Crohn's disease (23). The presence of these oligoclonal T-cell populations, including 'public' clones with identical rearrangements found in different patients, supports the notion that antigen-specific T-cell activation is a major pathogenetic mechanism of inflammation in these conditions. In patients with HLA-DR4^{+} rheumatoid arthritis, the TCR repertoire of T-cells responding to a major epitope of collagen was found restricted to a limited number of rearrangements that were shared between patients (50). In the peripheral blood of MS patients, the Vβ5.2 gene family was often oligoclonally expanded, while predominant TCR clones were stable over time but different from patient to patient (25). Stably expanded T-cell clones were also identified in skin lesions of patients with psoriasis vulgaris (26). In human SLE, besides the well-documented B-cell oligoclonality (51), also oligoclonal TCR repertoires have been repeatedly reported (29-31). Extensive sequencing has furthermore revealed that expanded T-cell clones persisted during disease inactivity, but became short-lived and highly volatile in periods of active disease (32).

Studying the effect of ivIg therapy on TCR repertoires in SLE patients, we have now found that their perturbation was relatively reduced under clinically successful ivIg therapy, supporting the notion that the beneficial effect of ivIg includes a stabilization of diversified TCR repertoires, as we have already described it in other contexts (6, 7). This result is principally robust against confounders such as possible intercurrent infections, since these could only increase but not reduce the repertoire perturbation. Without knowing to which extent expanded clones were pathogenic or not, we found that the individual repertoire perturbation under ivIg in two of four Vβ families studied (Vβ11 and Vβ14) was strongly correlated with the individual average surface CD25 density on Foxp3^{+} Tregs. This is in good agreement with the generally accepted evidence that Tregs control the proliferation and clonal expansion of conventional T-cells (14), and with the notion that CD25 (the IL-2 receptor α chain that enables high-affinity IL-2 binding) surface density indicates the relative activity of human Tregs. This is particularly well supported for SLE, where CD25^{+} or CD25^{bright} rather than total Foxp3^{+} Tregs were found deficient (15, 52-55), and more recently their reduced CD25 expression (17, 18) was directly associated to the previously described functional deficiency of Foxp3^{+} Tregs in SLE (16).

Our finding that repertoire diversity under ivIg treatment was significantly correlated with individual Treg surface CD25, thus likely with Treg activity (17, 18), does not exclude Treg-independent effects of ivIg that could also inhibit specific clonal expansion. However, this result strongly supports the hypothesis that under ivIg therapy Tregs substantially contribute to controlling and limiting expanded T-cell clones, likely including pathogenic ones, which (although we have no direct evidence for it) raises the possibility that also the therapeutic effect of ivIg could in part depend on functionally active CD25^{bright} Tregs that are present to different extents in individual patients. The alternative explanation, an impact of repertoire diversity on the individual Treg status, seems much more farfetched and is particularly difficult to reconcile with the relatively rapid changes that we detected over time in the same patients in repertoire diversity but not in Treg properties. The third theoretically possible explanation, a correlation of secondary effects due to a shared primary effect (ivIg), can be readily excluded since CD25 MFI, other than repertoire diversity, did not detectably depend on ivIg treatment in our study. The fact that the clinical nonresponders were equally well fitted suggests that the putative mechanism that linked active Tregs to repertoire diversity was present

also in this group, explainable by the possibility that disease activity was here driven by effects other than oligoclonal T-cell expansion that escaped T-cell regulation. It is furthermore interesting that the correlations of CD25 MFI with repertoire diversity under ivIg were similarly significant in both the $CD4^+CD45RO^+Foxp3^{bright}$ and $CD4^+CD45RO^+Foxp3^{low}$ Treg subsets. This supports the hypothesis that the latter, at least in SLE, represents a true Treg population as suggested (16, 17), and not merely activated conventional T-cells with transient low-grade Foxp3 expression (41). We do not know, however, if it has an informative value that only Vβ11 and Vβ14 diversity was significantly correlated with the expression of CD25 on Tregs. Since correlation coefficients with Treg CD25 (Table 2) were throughout negative also for Vβ1 and Vβ2, it is well possible that our interpretation principally also applies to them and that the different significances were due to sample bias. Still, it is also possible that effector T-cells bearing Vβ11 and Vβ14 are indeed overrepresented in SLE-associated autoimmune reactions and that Tregs accordingly suppressed them more than others.

In our study we did not find evidence that Treg properties depended on ivIg treatment. However, our study is certainly not sufficient to make any conclusion in this respect, and a Treg-mediated effect of ivIg has indeed previously been described in experimental autoimmune encephalomyelitis in mice (11). Also in human Kawasaki disease, where ivIg is an established therapy, its therapeutic effect was recently reported to be accompanied by the repair of a Treg deficit (13). Moreover, the study of bone marrow reconstitution has suggested an effect of ivIg on T-cell repertoires that included Tregs (6-8). In this condition, ivIg generally stimulates T-cells, likely by natural antigenicity included in the polyclonal immunoglobulin preparation (56). Indeed, Tregs, known in many ways and likely selected to recognize self antigens (57), were recently also found to be stimulated by major MHC class II-restricted epitopes in the Fc portion of human IgG, accordingly called 'Tregitopes' (10). The fact that we found no difference, both in cell number and CD25 expression, in the Treg compartment during ivIg therapy in our study, means that effects of ivIg on Tregs here either implied only a small subset of Tregs without detectably affecting the overall Treg status, or that other ivIg mechanisms played the principal role in the increased diversity of the T-cell repertoire. In the OVA-specific humoral immune response in mice, ivIg in fact rather interfered with the generation of antigen-specific T cells. Further in vitro experiments revealed that the effect of IvIg was mediated by APCs, resulting in an inhibition of upstream signals

provided by APCs that inhibited T-cell activation, proliferation, and cytokine secretion without ivIg directly interacting with T-cells (58). However, additional studies addressing the roles of the different effects of ivIg in humans are clearly required.

Conclusions

Our findings support an influence of Tregs on ivIg effects. This is in agreement with the interpretation that ivIg, besides its effects on Fc receptors and circulating antibodies, could protect a healthy and diverse T-cell repertoire from destabilizing effects also by providing natural antigenic stimuli, with an overall effect of limiting clonal expansion, thus 'buffering' natural T-cell repertoires.

Acknowledgments

References

1.      Arnson Y, Shoenfeld Y, Amital H. Intravenous immunoglobulin therapy for autoimmune diseases. Autoimmunity. 2009;42(6):553-60.

2.      Levy Y, Sherer Y, Ahmed A, Langevitz P, George J, Fabbrizzi F, et al. A study of 20 SLE patients with intravenous immunoglobulin - clinical and serologic response. Lupus. 1999;8(9):705-12.

3.      Zandman-Goddard G, Blank M, Shoenfeld Y. Intravenous immunoglobulins in systemic lupus erythematosus: from the bench to the bedside. Lupus. 2009;18(10):884-8.

4.      Nimmerjahn F, Ravetch JV. Antibody-mediated modulation of immune responses. Immunol Rev. 2010;236:265-75.

5.      Smith KGC, Clatworthy MR. Fc gamma RIIB in autoimmunity and infection: evolutionary and therapeutic implications. Nat Rev Immunol. 2010 May;10(5):328-43.

6.      Joao C, Ogle BM, Gay-Rabinstein C, Platt JL, Cascalho M. B Cell-dependent TCR diversification. J Immunol. 2004;172(8):4709-16.

7.      Joao C, Ogle BM, Geyer S. Immunoglobulin promotes the diversity and the function of T cells. Eur J Immunol. 2006;36(7):1718-28.

8.      Pires AE, Afonso AF, Queiros A, Cabral MS, Porrata L, Markovic SN, et al. Treatment With Polyclonal Immunoglobulin During T-cell Reconstitution Promotes Naive T-cell Proliferation. J Immunother. 2010;33(6):618-25.

9.      Kessel A, Ammuri H, Peri R, Pavlotzky ER, Blank M, Shoenfeld Y, et al. Intravenous immunoglobulin therapy affects T regulatory cells by increasing their suppressive function. J Immunol. 2007;179:5571-5.

10.     De Groot AS, Moise L, McMurry JA, Wambre E, Van Overtvelt L, Moingeon P, et al. Activation of natural regulatory T cells by IgG Fc-derived peptide "Tregitopes". Blood. 2008;112(8):3303-11.

11.     Ephrem A, Chamat S, Miquel C, Fisson S, Mouthon L, Caligiuri G, et al. Expansion of CD4(+)CD25(+) regulatory T cells by intravenous immunoglobulin: a critical factor in controlling experimental autoimmune encephalomyelitis. Blood. 2008;111(2):715-22.

12.     Maddur MS, Othy S, Hegde P, Vani J, Lacroix-Desmazes S, Bayry J, et al. Immunomodulation by Intravenous Immunoglobulin: Role of Regulatory T Cells. J Clin Immunol. 2010;30:S4-S8.

13.     Olivito B, Taddio A, Simonini G, Massai C, Ciullini S, Gambineri E, et al. Defective FOXP3 expression in patients with acute Kawasaki disease and restoration by intravenous immunoglobulin therapy. Clin Exp Rheumatol. 2010;28(1 Suppl 57):93-7.

14.     Sakaguchi S, Miyara M, Costantino CM, Hafler DA. FOXP3(+) regulatory T cells in the human immune system. Nat Rev Immunol. 2010;10(7):490-500.

15.     Scheinecker C, Bonelli M, Smolen JS. Pathogenetic aspects of systemic lupus erythematosus with an emphasis on regulatory T cells. J Autoimmun. 2010;35(3):269-75.

16.     Valencia X, Yarboro C, Illei G, Lipsky PE. Deficient CD4(+)CD25(high) T regulatory cell function in patients with active systemic lupus erythematosus. J Immunol. 2007 Feb 15;178(4):2579-88.

17.     Bonelli M, Savitskaya A, Steiner CW, Rath E, Smolen JS, Scheinecker C. Phenotypic and Functional Analysis of CD4(+)CD25(-)Foxp3(+) T Cells in Patients with Systemic Lupus Erythematosus. J Immunol. 2009;182(3):1689-95.

18.     Horwitz DA. Identity of mysterious CD4(+)CD25(-)Foxp3(+) cells in systemic lupus erythematosus. Arthritis Res Ther. 2010;12(1):201.

19.     Zheng L, Sharma R, Kung JT, Deshmukh US, Jarjour WN, Fu SM, et al. Pervasive and stochastic changes in the TCR repertoire of regulatory T-cell-deficient mice. Int Immunol. 2008;20(4):517-23.

20.     Zennaro D, Scala E, Pomponi D, Caprini E, Arcelli D, Gambineri E, et al. Proteomics plus genomics approaches in primary immunodeficiency: the case of immune dysregulation, polyendocrinopathy, enteropathy, X-linked (IPEX) syndrome. Clin Exp Immunol. 2012;167(1):120-8.

21.     Pannetier C, Cochet M, Darche S, Casrouge A, Zoller M, Kourilsky P. The sizes of the CDR3 hypervariable regions of the murine T-cell receptor beta-chains vary as a function of the recombined germ-line segments. Proc Natl Acad Sci USA. 1993;90(9):4319-23.

22.     Fitzgerald JE, Ricalton NS, Meyer AC, West SG, Kaplan H, Behrendt C, et al. Analysis of clonal CD8(+) T-cell expansions in normal individuals and patients with rheumatoid arthritis. J Immunol. 1995;154(7):3538-47.

23.     Gulwani-Akolkar B, Akolkar PN, Minassian A, Pergolizzi R, McKinley M, Mullin G, et al. Selective expansion of specific T cell receptors in the inflamed colon of Crohn's disease. J Clin Invest. 1996;98(6):1344-54.

24.     Wagner UG, Koetz K, Weyand CM, Goronzy JJ. Perturbation of the T cell

repertoire in rheumatoid arthritis. Proc Natl Acad Sci USA. 1998;95(24):14447-52.

25.    Matsumoto Y, Yoon WK, Jee Y, Fujihara K, Misu T, Sato S, et al. Complementarity-determining region 3 spectratyping analysis of the TCR repertoire in multiple sclerosis. J Immunol. 2003;170(9):4846-53.

26.    Diluvio L, Vollmer S, Besgen P, Ellwart JW, Chimenti S, Prinz JC. Identical TCR beta-chain rearrangements in streptococcal angina and skin lesions of patients with psoriasis vulgaris. J Immunol. 2006;176(11):7104-11.

27.    Matsumoto Y, Matsuo H, Sakuma H, Park IK, Tsukada Y, Kohyama K, et al. CDR3 spectratyping analysis of the TCR repertoire in myasthenia gravis. J Immunol. 2006;176(8):5100-7.

28.    Olive C, Gatenby PA, Serjeantson SW. Restricted junctional diversity of T-cell receptor delta-gene rearrangements expressed in systemic lupus erythematosus (SLE) patients. Clin Exp Immunol. 1994;97(3):430-8.

29.    Holbrook MR, Tighe PJ, Powell RJ. Restrictions of T cell receptor beta chain repertoire in the peripheral blood of patients with systemic lupus erythematosus. Ann Rheum Dis. 1996;55(9):627-31.

30.    Kolowos W, Herrmann M, Ponner BB, Voll R, Kern P, Frank C, et al. Detection of restricted junctional diversity of peripheral T cells in SLE patients by spectratyping. Lupus. 1997;6(9):701-7.

31.    Fraser PA, Lu LY, DeCeulaer K, Schur PH, Fici D, Awdeh Z, et al. CD4 TCRBV CDR3 analysis in prevalent SLE cases from two ethnic groups. Lupus. 1999;8(4):311-9.

32.    Kato T, Kurokawa M, Sasakawa H, Masuko-Hongo K, Matsui T, Sekine T, et al. Analysis of accumulated T cell clonotypes in patients with systemic lupus erythematosus. Arthritis Rheum. 2000;43(12):2712-21.

33.    Massengill SF, Goodenow MM, Sleasman JW. SLE nephritis is associated with an oligoclonal expansion of intrarenal T cells. Am J Kidney Dis. 1998;31(3):418-26.

34.    Collette A, Six A. ISEApeaks: an Excel platform for GeneScan and Immunoscope data retrieval, management and analysis. Bioinformatics. 2002;18(2):329-30.

35.    Collette A, Cazenave PA, Pied S, Six A. New methods and software tools for high throughput CDR3 spectratyping. Application to T lymphocyte repertoire modifications during experimental malaria. J Immunol Meth. 2003;278(1-2):105-16.

36.    Gorochov G, Neumann AU, Kereveur A, Parizot C, Li TS, Katlama C, et al.

Perturbation of CD4(+) and CD8(+) T-cell repertoires during progression to AIDS and regulation of the CD4(+) repertoire during antiviral therapy. Nat Med. 1998;4(2):215-21.

37.	Han M, Harrison L, Kehn P, Stevenson K, Currier J, Robinson MA. Invariant or highly conserved TCR alpha are expressed on double-negative (CD3(+)CD4(-)CD8(-)) and CD8(+) T cells. J Immunol. 1999;163(1):301-11.

38.	Rosner B. A Generalization of the Paired t-Test. Appl Statist. 1982;31(1):9-13.

39.	Press W. Numerical Recipes in C. Cambridge: Cambridge University Press; 1994.

40.	R development Core Team. R: A language and environment for statistical computing. Vienna: R Foundation for Statistical Computing; 2012.

41.	Miyara M, Yoshioka Y, Kitoh A, Shima T, Wing K, Niwa A, et al. Functional Delineation and Differentiation Dynamics of Human CD4(+) T Cells Expressing the FoxP3 Transcription Factor. Immunity. 2009;30(6):899-911.

42.	Lawson TM, Man S, Williams S, Boon ACM, Zambon M, Borysiewicz LK. Influenza A antigen exposure selects dominant V(beta)17(+) TCR in human CD8(+) cytotoxic T cell responses. Int Immunol. 2001 Nov;13(11):1373-81.

43.	Turner SJ, Doherty PC, McCluskey J, Rossjohn J. Structural determinants of T-cell receptor bias in immunity. Nat Rev Immunol. 2006 Dec;6(12):883-94.

44.	Gras S, Kjer-Nielsen L, Burrows SR, McCluskey J, Rossjohn J. T-cell receptor bias and immunity. Curr Opin Immunol. 2008 Feb;20(1):119-25.

45.	Miles JJ, Thammanichanond D, Moneer S, Nivarthi UK, Kjer-Nielsen L, Tracy SL, et al. Antigen-Driven Patterns of TCR Bias Are Shared across Diverse Outcomes of Human Hepatitis C Virus Infection. J Immunol. 2011 Jan 15;186(2):901-12.

46.	Roux E, Dumont-Girard F, Starobinski M, Siegrist CA, Helg C, Chapuis B, et al. Recovery of immune reactivity after T-cell-depleted bone marrow transplantation depends on thymic activity. Blood. 2000;96(6):2299-303.

47.	Hirokawa M, Matsutani T, Horiuchi T, Kawabata Y, Kitabayashi A, Yoshioka T, et al. Extensive clonal expansion of T lymphocytes causes contracted diversity of complementarity-determining region 3 and skewed T cell receptor repertoires after allogeneic hematopoietic cell transplantation. Bone Marrow Transplantation. 2001;27(6):607-14.

48.	Talvensarri K, Clave E, Douay C, Rabian C, Garderet L, Busson M, et al. A broad T-cell repertoire diversity and an efficient thymic function indicate a favorable

long-term immune reconstitution after cord blood stem cell transplantation. Blood. 2002;99(4):1458-64.

49. Kou ZC, Puhr JS, Wu SS, Goodenow MM, Sleasman JW. Combination Antiretroviral therapy results in a rapid increase in T cell receptor variable region beta repertoire diversity within CD45RA CD8 T cells in human immunodeficiency virus-infected children. J Infect Dis. 2003;187(3):385-97.

50. Ria F, Penitente R, De Santis M, Nicolo C, Di Sante G, Orsini M, et al. Collagen-specific T-cell repertoire in blood and synovial fluid varies with disease activity in early rheumatoid arthritis. Arthritis Res Ther. 2008;10(6):R135.

51. Jacobi AM, Diamond B. Balancing diversity and tolerance: lessons from patients with systemic lupus erythematosus. J Exp Med. 2005;202(3):341-4.

52. Crispin JC, Martinez A, Alcocer-Varela J. Quantification of regulatory T cells in patients with systemic lupus erythematosus. J Autoimmun. 2003 Nov;21(3):273-6.

53. Liu MF, Wang CR, Fung LL, Wu CR. Decreased CD4+CD25+ T cells in peripheral blood of patients with systemic lupus erythematosus. Scand J Immunol. 2004;59:198-202.

54. Miyara M, Amoura Z, Parizot C, Badoual C, Dorgham K, Trad S, et al. Global natural regulatory T cell depletion in active systemic lupus erythematosus. J Immunol. 2005;175(12):8392-400.

55. Lee JH, Wang LC, Lin YT, Yang YH, Lin DT, Chiang BL. Inverse correlation between CD4+ regulatory T-cell population and autoantibody levels in paediatric patients with systemic lupus erythematosus. Immunology. 2006;117:280-6.

56. Joao C. Immunoglobulin is a highly diverse self-molecule that improves cellular diversity and function during immune reconstitution. Med Hypotheses. 2007;68(1):158-61.

57. Pacholczyk R, Kern J. The T-cell receptor repertoire of regulatory T cells. Immunology. 2008;125(4):450-8.

58. Aubin E, Lemieux R, Bazin R. Indirect inhibition of in vivo and in vitro T-cell responses by intravenous immunoglobulins due to impaired antigen presentation. Blood. 2010 Mar 4;115(9):1727-34.

Figure Legends

**Fig. 1** TCR CDR3 Vβ1, Vβ2, Vβ11 and Vβ14 spectratype profiles of patient F3 before and during ivIg therapy. Each column corresponds to the indicated Vβ family. Each row corresponds to a time point relative to the first ivIg infusion, expressed in days: D000 is the initial sample collected before ivIg treatment. Each panel depicts the distribution of amplified CDR3 fragment sizes, with the X axis representing an appropriately defined range of sizes for each Vβ family. Each peak represents a defined CDR3 length. The number in each panel insert, ranging from 0 to 100, is the perturbation index calculated at each time point in respect to patient F3's average profile for the respective Vβ family.

**Fig. 2** Average TCR CDR3 perturbations are decreased in patients successfully treated with ivIg. TCR CDR3 perturbation indexes, as shown in Fig. 1 for patient F3, were determined for all patients, time points and Vβ families. Average perturbation scores were calculated for each patient and Vβ (a) for the time points under ivIg treatment (black bars) and (b) for those outside ivIg treatment (grey bars). Patients are indicated by their codes on the x axis. Patients who did not respond clinically to a therapy cycle are indicated with a star. The number of total samples obtained from each patient is annotated in brackets, e.g.: LI1 (20 samples under ivIg + 6 outside ivIg treatment).

**Fig. 3** Individual evolutions of TCR CDR3 perturbations in six patients treated with ivIg. Each panel represents one patient. The Vβ families are indicated in each panel by different line styles: Vβ1 dotted, Vβ2 dashed, Vβ11 solid, Vβ14 dotted and dashed. Arrows at the bottom of each panel mark the time periods when the respective patient was under ivIg treatment: full arrows indicate treatment cycles with clinical improvement, dashed arrows cycles without clinical improvement.

**Fig. 4** Representative cytometric profile of Foxp3 and CD45RO staining (gated on CD4+ T-cells). Gates R5-R6 indicate the analyzed subpopulations of Foxp3+ T-cells: $Foxp3^{low}CD45RO+$ (R5, described as nonsuppressive); $Foxp3^{high}CD45RO+$ (R6, activated Tregs); Foxp3+CD45RO- (R7, 'resting' Tregs).

**Fig. 5** SLE patients had reduced CD25 surface densities on Tregs. CD25 surface densities on CD4+Foxp3+ Tregs were compared between ivIg-treated SLE patients and healthy blood donors (controls), considering all time points where CD25 quantification was available. The insert shows the P-value obtained by a distribution-independent Mann-Whitney test.


**Fig. 6** Correlations between average CD25 surface density on Foxp3+ Tregs and Vβ11 and Vβ14 average perturbations in patients under ivIg treatment. Each dot represents a patient and is annotated with the corresponding patient-code. Inserts indicate Spearman rank correlation coefficients and corresponding p-values.

**Table 1. Patients studied**

| Patient | Diagnosis | Age | Gender | Indication | Therapy apart from IvIg[b] | IvIg infusions followed | SLEDAI before IvIg | Clinical improvement under IvIg | Number of samples analyzed | Number of samples under IvIg | Number of samples outside IvIg |
|---|---|---|---|---|---|---|---|---|---|---|---|
| L11[a] | Discoid LE | 46 | F | Cutaneous Flare | HCQ 400 | 12 | 23/21 | Yes/Yes | 28 | 20 | 6 |
| F2[a] | SLE | 44 | F | Cutaneous Flare | PRD 90, AZA in second cycle | 9 | 14/14 | Yes/No | 13 | 8 | 4 |
| F1 | SLE | 56 | F | Systemic Flare | PRD 90 | 6 | 16 | Yes | 6 | 4 | 1 |
| F3 | SLE | 19 | F | Systemic Flare | DFL 30 | 6 | 7 | Yes | 8 | 6 | 1 |
| F4 | SLE | 32 | M | Flare w. Thrombocytopenia | PRD 150 | 6 | 5 | No | 8 | 6 | 2 |
| F6 | SLE | 48 | F | Systemic flare | DFL 15 | 6 | 17 | Yes | 6 | 4 | 1 |
| F8 | SLE | 17 | F | Flare w. Thrombocytopenia | None | 6 | 3 | Yes | 5 | 4 | 1 |
| FA1 | SLE | 53 | F | Systemic Flare | None | 3 | 20 | Yes | 7 | 5 | 1 |
| G1 | SLE | 47 | F | Cutaneous Flare | MTX | 2 | 2 | No | 3 | 1 | 1 |
| P92 | SLE | 36 | F | Systemic and cut. Flare | PRD 10, AZA | 6 | 25 | Yes | 7 | 5 | 2 |
| P97 | SLE | 49 | F | Cutaneous Flare | PRD 10 | 6 | 4 | Yes | 8 | 5 | 3 |
| P150 | SLE | 49 | F | Cutaneous Flare | PRD 10, MTX | 2 | 4 | No | 4 | 2 | 2 |
| P163 | SLE | 33 | F | Cutaneous Flare | PRD 5, MTX | 3 | 2 | Yes | 7 | 3 | 3 |
| P230 | SLE | 21 | F | Cutaneous Flare | PRD 12.5, AZA | 4 | 4 | No | 3 | 1 | 2 |
| V1 | SLE | 34 | F | Cut. Flare and incr. anti-DNA | PRD 20, MTX | 2 | 12 | Yes | 7 | 5 | 1 |

[a]Received two consecutive cycles of ivIg therapy

[b]HCQ=Hydroxychloroquine, DFL=Deflazacort, PRD=Prednisone, AZA=Azathioprine, MTX=Methotrexate, doses in mg/day

24

**Table 2. Spearman correlations[a] and weighted least squares regression[b] of individually averaged Foxp3+ Treg frequencies and log-MFI(CD25) in Tregs and T-cell subsets versus BV familywise perturbation under ivIg treatment**

| | BV1[a] | BV1[b] | BV2[a] | BV2[b] | BV11[a] | BV11[b] | BV14[a] | BV14[b] |
|---|---|---|---|---|---|---|---|---|
| Frequency of Foxp3+ in CD4+ | -.35(.27) | (.17) | -.31(.27) | (.61) | -.11(.69) | (.49) | +.01(.98) | (.99) |
| log-MFI(CD25) in all CD4+Foxp3+ | -.21(.51) | (.29) | -.32(.24) | (.21) | **-.77(.006)** | **(.0007)** | **-.61(.027)** | **(.005)** |
| log-MFI(CD25) in CD4+Foxp3$^{high}$CD45RO+ | -.42(.19) | (.42) | -.26(.35) | (.33) | **-.58(.036)** | **(.048)** | **-.75(.007)** | **(.0008)** |
| log-MFI(CD25) in CD4+Foxp3$^{low}$CD45RO+ | -.36(.25) | (.21) | -.31(.26) | (.17) | **-.83(.003)** | **(6E-5)** | **-.61(.027)** | **(.005)** |
| log-MFI(CD25) in CD4+Foxp3+CD45RO- | -.06(.84) | (.72) | -.08(.77) | (.62) | -.42(.13) | (.12) | -.26(.35) | (.31) |
| log-MFI(CD25) in CD4+Foxp3-CD45RO+ | -.33(.30) | (.18) | -.12(.67) | (.74) | -.40(.15) | (.07) | +.04(.89) | (.98) |
| log-MFI(CD25) in CD4+Foxp3-CD45RO- | -.23(.47) | (.20) | +.22(.43) | (.69) | -.15(.59) | (.19) | +.23(.40) | (.71) |

[a]Spearman R (in brackets: P-value). [b](P-value) calculated with N$^{1/2}$ as weights (N: individual sample number).

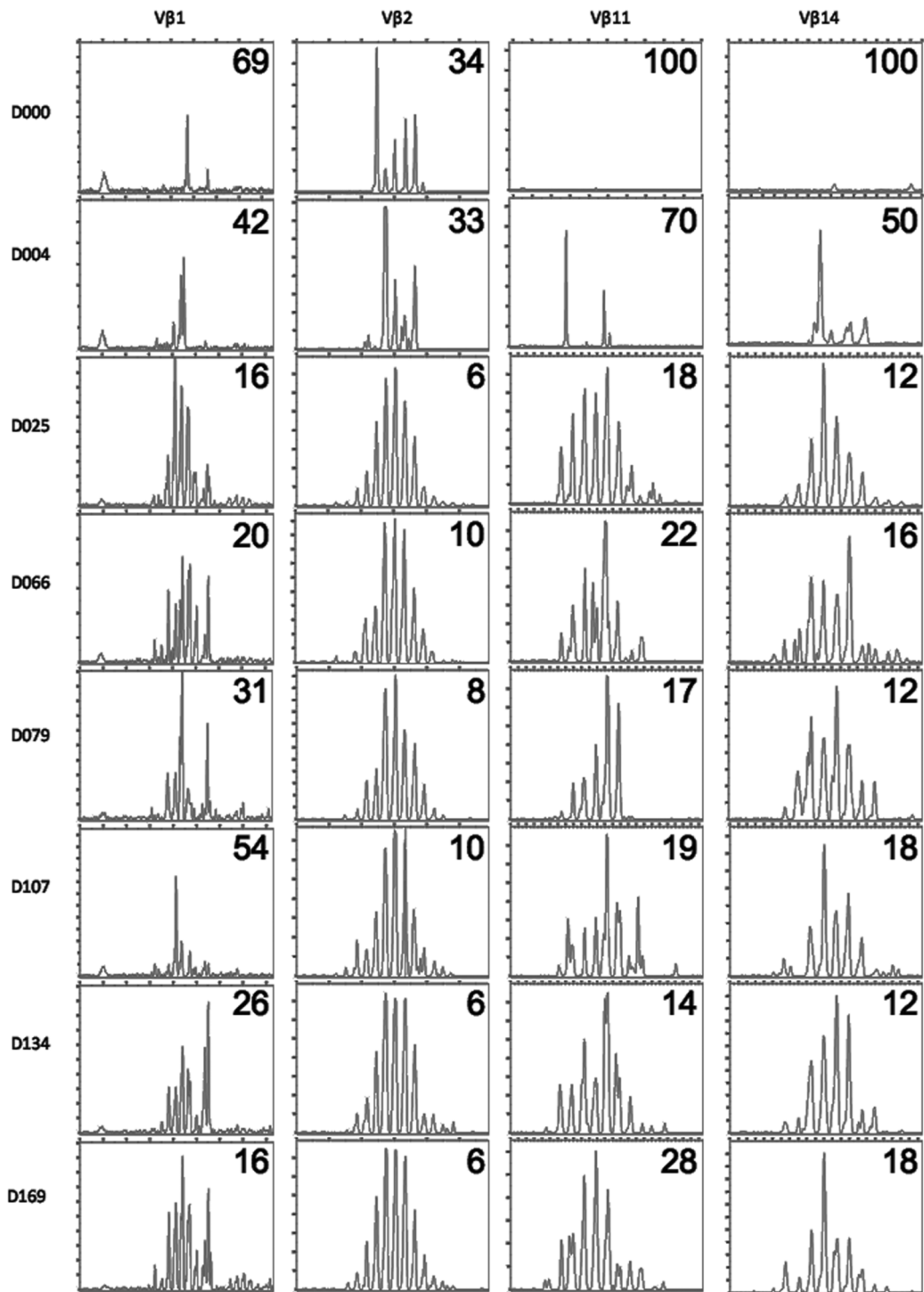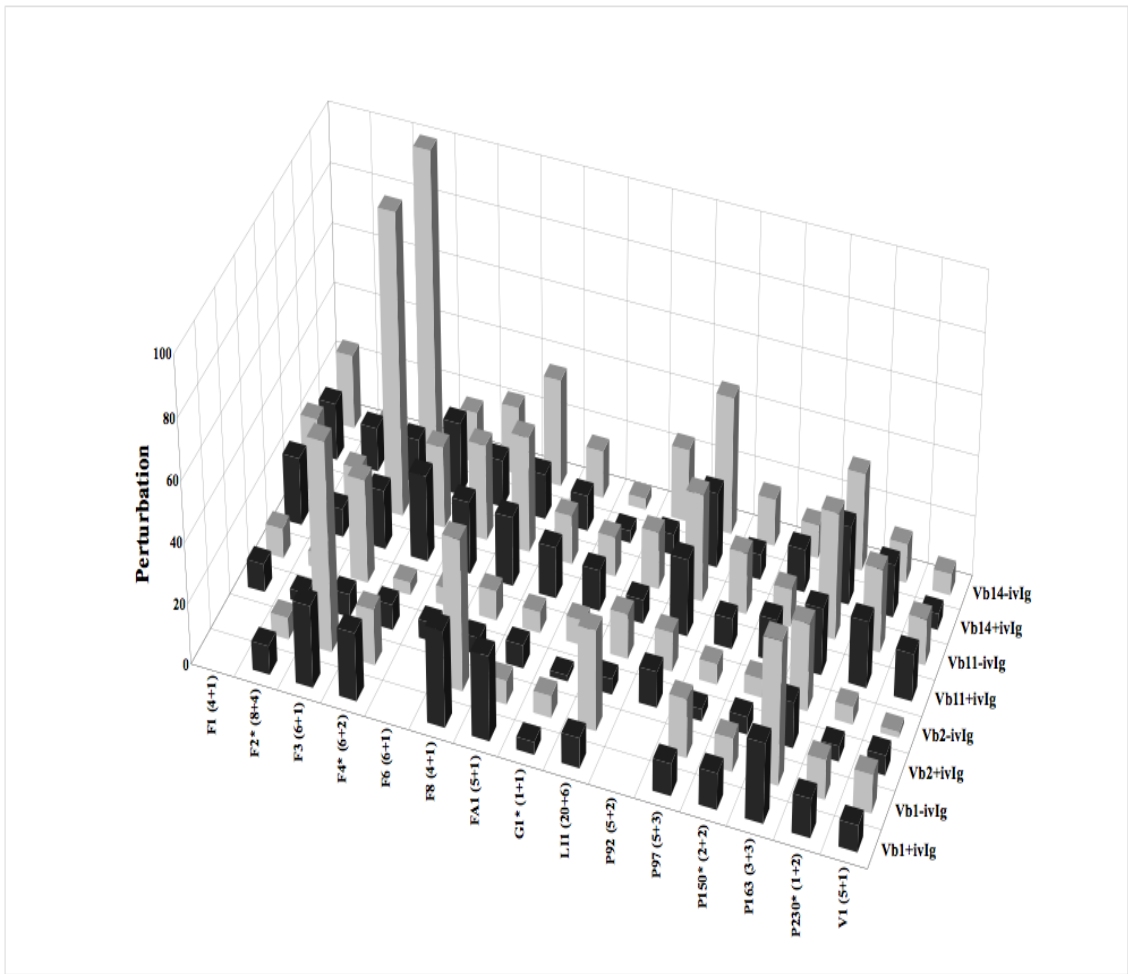Statistically significant values are shown in bold type.
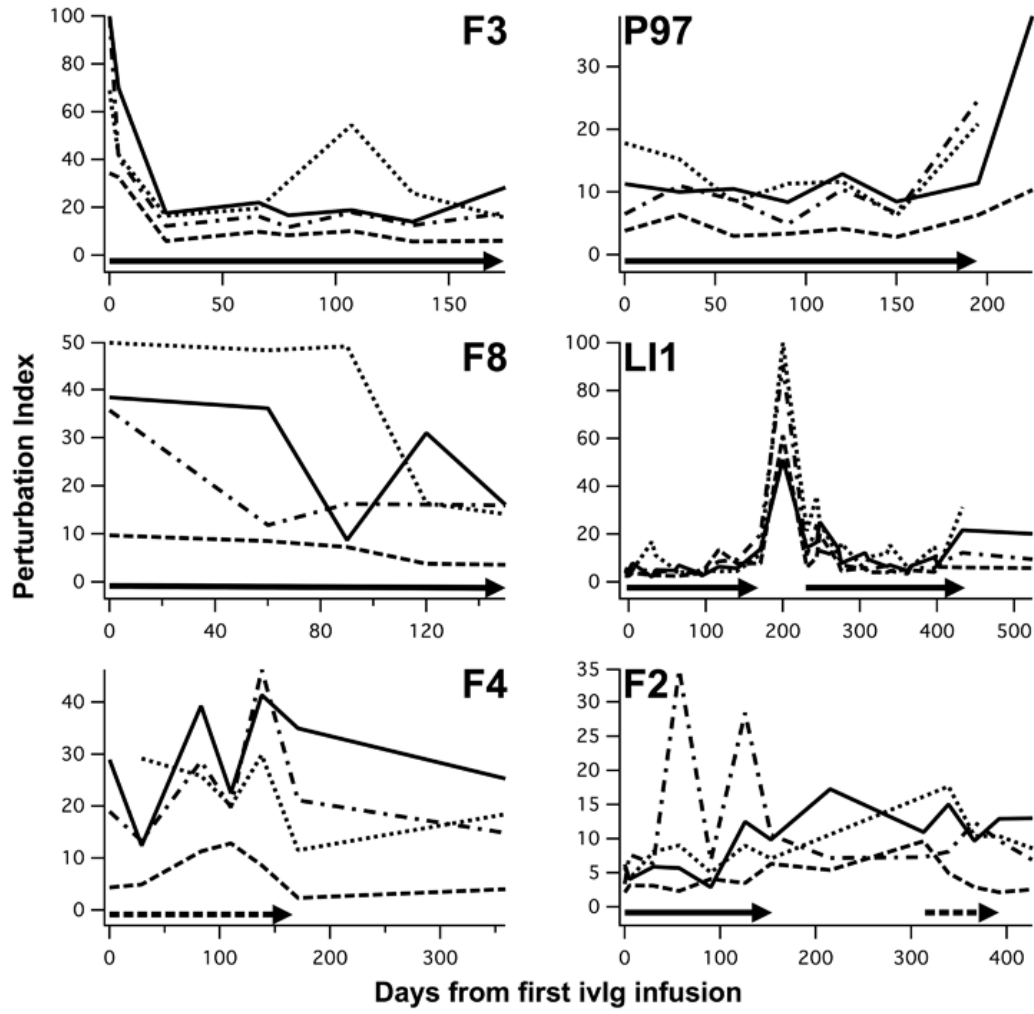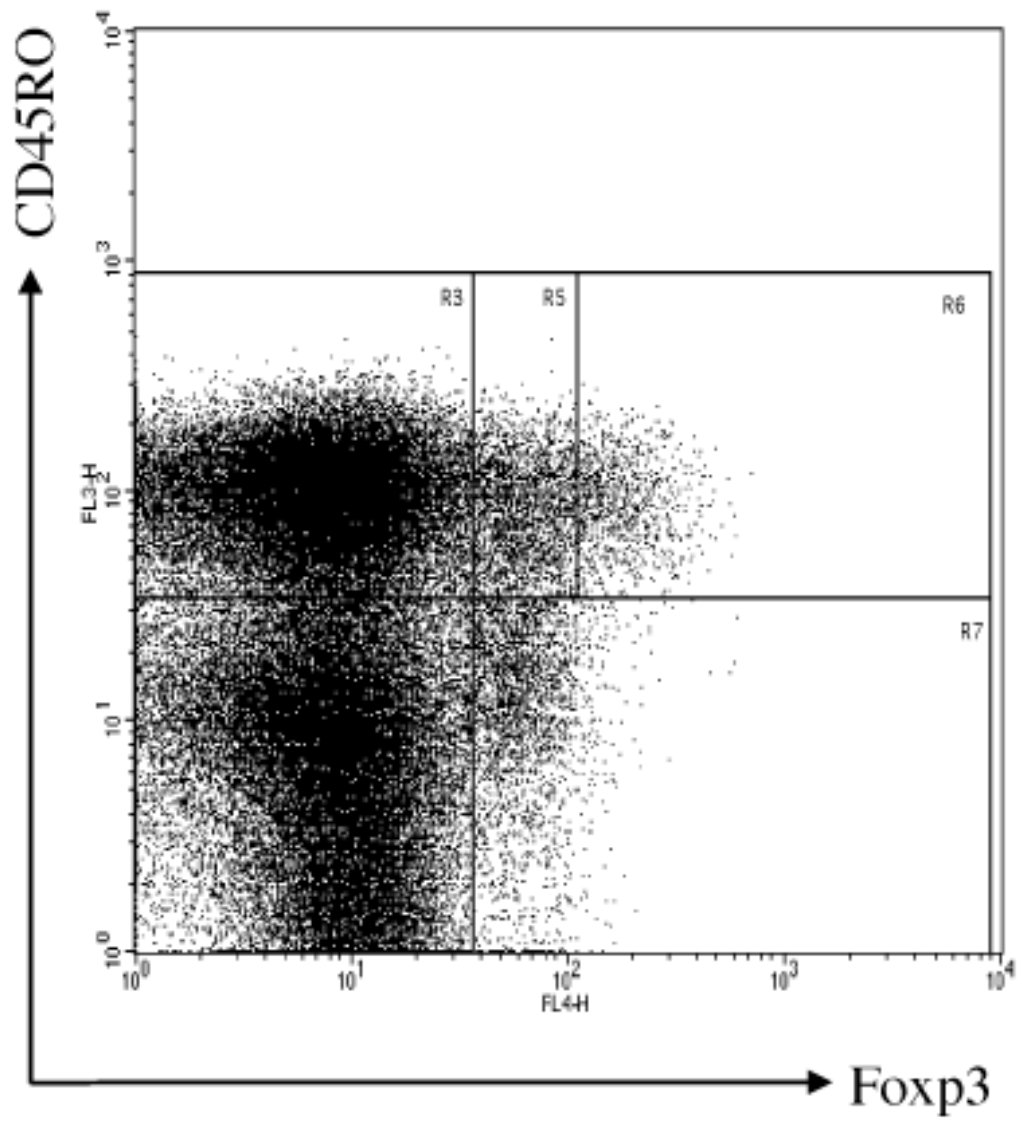
Fig 1
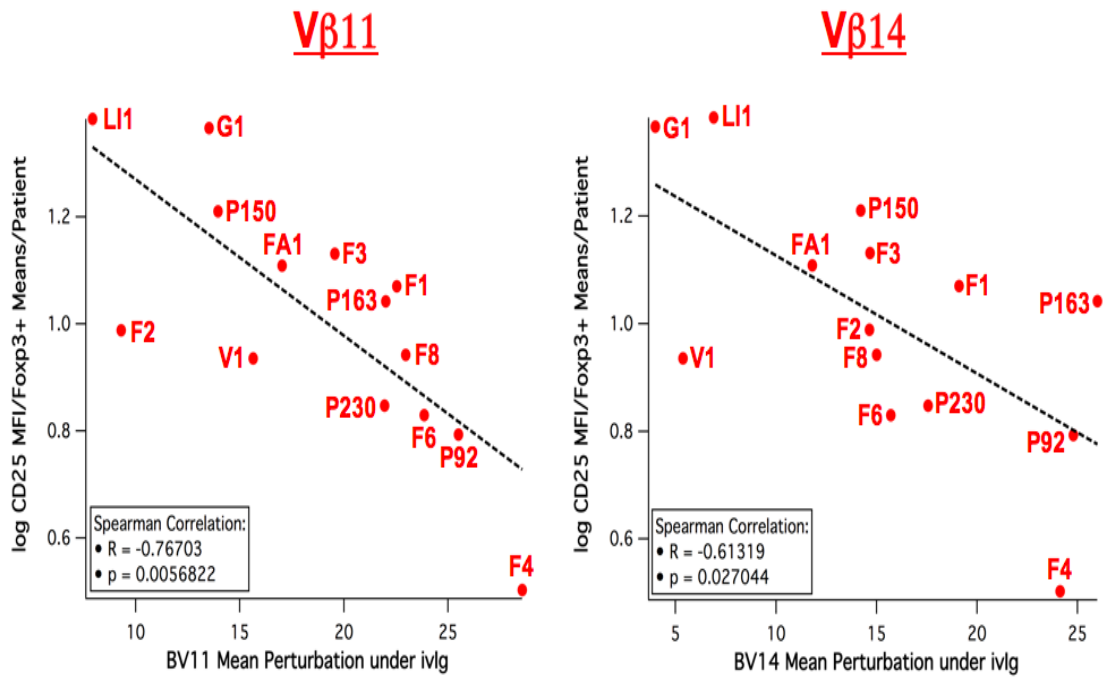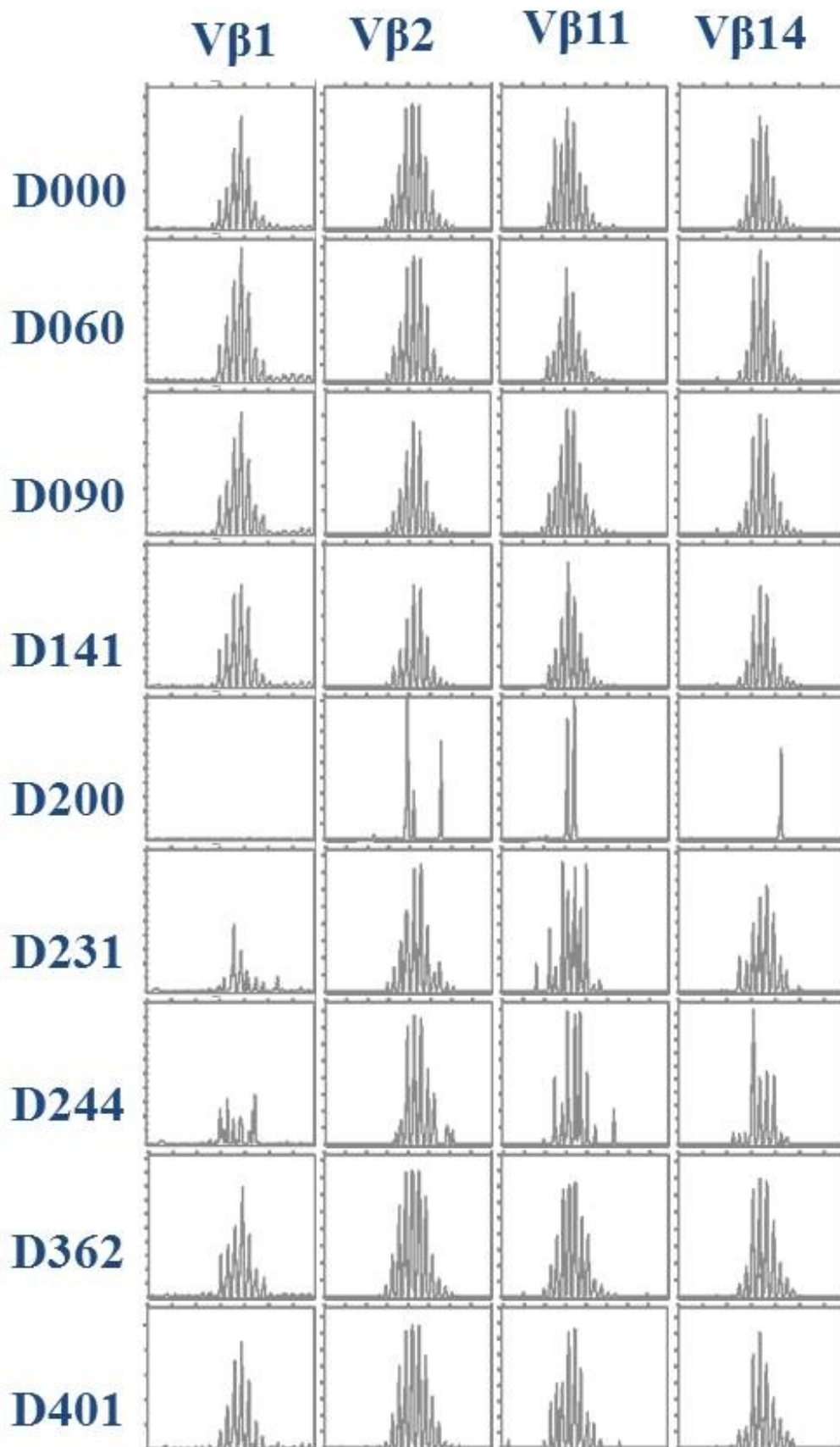
Fig 2

Fig 3

Fig 4

Fig 5

Fig 6

Fig S1 TCR CDR3 profiles of patient LI1 at various time points (analogously to Fig. 1)
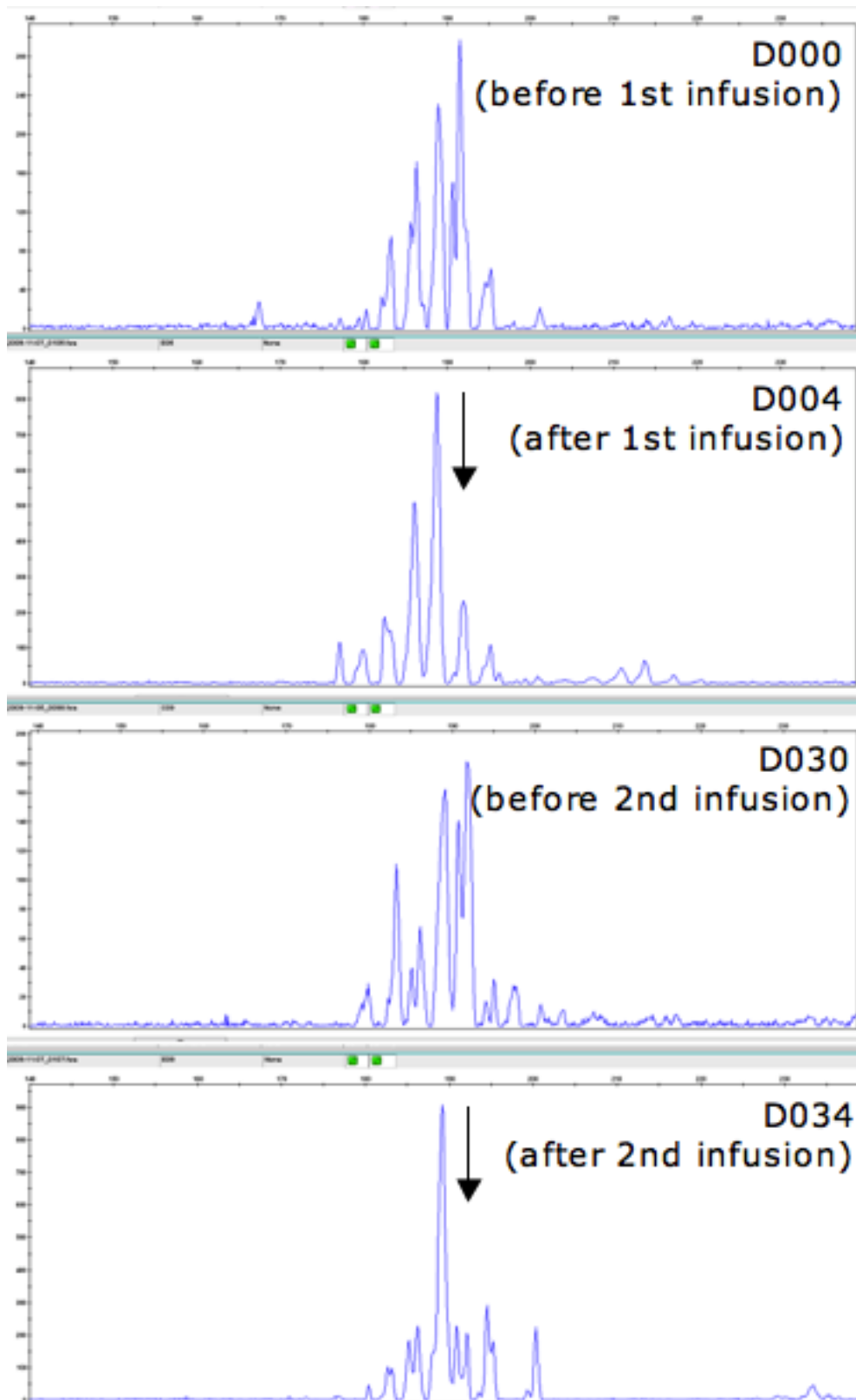
Fig S2

TCR CDR3 V!1 profiles in patient FA1 before and after 1st and 2nd ivIg infusions
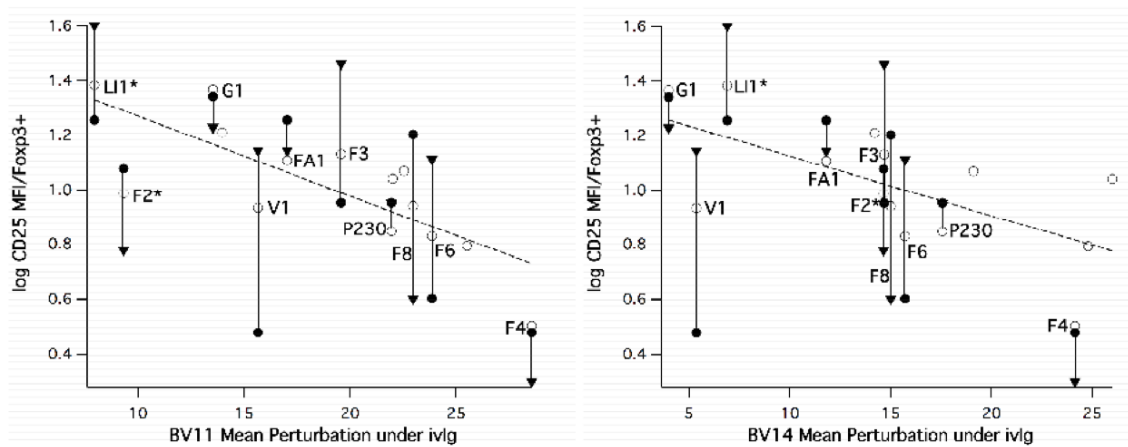
Fig. S3 Individual pre-ivIg and post-ivIg CD25 MFI of Foxp3+ Tregs in relation to V!11 and V!14 average perturbation under ivIg. For those patients where individual cytometric pre- and post-ivIg CD25 MFI measures were available, they are shown analogously to Fig. 6. Filled circles indicate pre-ivIg, triangles post-ivIg measures and open circles averages as shown in Fig. 6, on which also the regression line was calculated. *For LI1 and F2, pre-ivIg values represent the time before initiation of the respective second ivIg cycle of these patients.